Thermochimica Acta, 226 (1993) 33–42
Elsevier Science Publishers B.V., Amsterdam

Thermally stimulated creep (TSCr) study of polyamide 66 and polyamide 66/EPR blends [1]

M. Diffalah, Ph. Demont * and C. Lacabanne

Laboratoire de Physique des Solides (URA/CNRS/74), Université Paul Sabatier, 31062 Toulouse Cédex (France)

(Received 20 November 1992; accepted 14 May 1993)

Abstract

Thermally Stimulated Creep (TSCr) spectrometry with fractional loading (FL) has been used to investigate the relaxation processes of polyamide 66/EPR blends. According to the criteria of Starkweather, the γ- and β-retardation modes have been assigned to localized non-cooperative movements. No significant modifications of their fine structure are observed. The α_E-process, occuring in PA 66/EPR blends, and associated with the EPR glass transition, exhibits a cooperative feature. The scanning nature of the fractional loading method for the α-process has revealed two distributions of activation enthalpies corresponding to wet ambient and partially dry PA 66, respectively. The same behaviour is observed in PA 66/EPR blends.

INTRODUCTION

Most of the widely used thermoplastic materials, such as polyamides, show marked limitations in their use when toughness and high impact strength are required [1].

Polyamide 66 shows poor impact strength especially at temperatures below T_g and in the dry state. These limitations are overcome by melt-mixing these materials with a rubber-toughening agent. Of the many different types of elastomers that have been tested for rubber thoughening of polyamides, ethylene–propylene diene terpolymer (EPDM) and ethylene–propylene copolymer (EPR) are amongst the most sucessful [1–4]. The EPDM and EPR rubbers are treated with maleic anhydride (MAH) to provide reactive sites along the chain and then melt-blended with polyamide. Reactions of the maleic anhydride with the NH_2 end-groups of polyamide produce graft copolymers which aid dispersion and enhance interfacial adhesion.

* Corresponding author
[1] Presented at the 21st Annual NATAS Conference, Atlanta, GA, 13–16 September 1992.

0040-6031/93/$06.00 © 1993 – Elsevier Science Publishers B.V. All rights reserved

It has been shown by some authors [5–7] that there is a significant correlation between high impact strength and the dynamic mechanical losses which exist in the temperature and frequency range of the impact test, and which can dissipate the impact energy.

Therefore, thermally stimulated creep (TSCr) was applied to elucidate the relationships between mechanical relaxations and toughness in polyamide 66/EPR blends. The low equivalent frequency of TSCr ($f_{eq} = 10^{-4}$–10^{-3} Hz) leads to enhanced resolution of the different relaxation processes. The high resolving power of fractional loading (FL) was used to develop a better understanding of the nature of the distributions of retardation times in viscoelastic retardation processes of polyamide blends. These distributions are determined from the corresponding distributions of the activation enthalpies and activation entropies.

EXPERIMENTAL PROCEDURE

Materials

The series of samples under investigation were prepared and characterized by the Centre de Recherches de Saint-Fons/France/Rhône-Poulenc Recherches. The polyamide 66 (PA 66) (tradename AP 203) has a number average molecular weight $\bar{M}n$ of 16000 and a crystallinity of 35%, as determined by DSC.

The compositions of the blends were 94/6, 87/13 and 80/20 wt.% PA 66/EPR, denoted EPR 6, EPR 13 and EPR 20. Binary PA 66/EPR blends were prepared by melt-mixing in a twin-screw extruder at 275°C. They were injection-moulded into sheets (100 mm × 100 mm × 0.8 mm). Rectangular specimens (60 mm × 6 mm × 0.8 mm) where cut parallel to the injection direction and stored at ambient humidity for two months. The water content absorbed by PA 66 was 2.2 wt.%.

Method

Figure 1 outlines the principle of TSCr spectrometry [8–10]. The samples were cooled (for low-temperature (LT) TSCr complex spectra) or heated (for high-temperature (HT) TSCr complex spectra) from room temperature to a temperature T_σ. A static shear stress σ_0 was applied for Δt_σ ($\Delta t_{\sigma(LT)} = 6$ min and $\Delta t_{\sigma(HT)} = 2$ min). The samples were then quenched from T_σ to $T_o \ll T_\sigma$ ($T_{o(LT)} = -180$°C and $T_{o(HT)} = -25$°C), thus freezing-in mechanical strain γ_0. At T_o, the stress was removed. The samples were then heated in a slow and controlled manner up to T_σ at a rate b of 7°C min^{-1}. As the specimens were heated, the release of the frozen-in strain $\gamma(t)$ was recorded. Differentiation of $\gamma(t)$ was recorded, which yielded the rate of

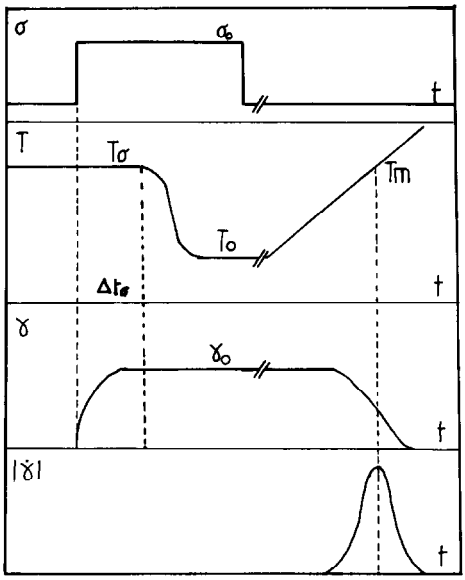

Fig. 1. The principle of thermally-stimulated creep (TSCr): the course of a TSCr experiment is shown as a schematic plot of applied stress σ_o, temperature T of the sample, strain γ and strain rate $|\dot{\gamma}|$ as a function of time.

release of recovery strain $\dot{\gamma}(t)$. All measurements were made in the linear region at strains $\gamma \leq 10^{-3}$. The temperature dependence of the TSCr recovery rate $\dot{\gamma}(T)$ was normalized to the applied shear stress to obtain thermally stimulated creep complex spectra.

The technique of fractional loading (FL) (Fig. 2) was used to resolve the TSCr complex spectra into elementary TSCr spectra. In FL experiments, a narrow packet of the distribution of retardation times is stimulated by an

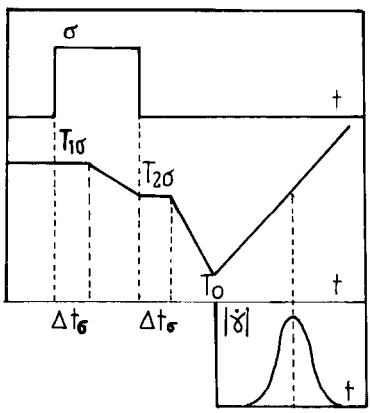

Fig. 2. Procedure of fractional loading (FL) in a TSCr experiment.

imposed mechanical stress history. The recovery kinetics of this narrow packet of relaxation times is then recorded experimentally. The experiments are performed with the same equipment as for the complex spectra. The time t, temperature T, and static shear stress σ program for a thermally fractional loading (FL) experiment is given in Fig. 2.

$T_{1\sigma} - T_{2\sigma} = \Delta T_\sigma$ is the stress window and the temperature difference between two successive applications of stress is the loading step. FL experiments are performed as follows: a stress σ is applied at $T_{1\sigma}$ for a time $\Delta t_\sigma = 2$ min; the temperature is then lowered by ΔT to $T_{2\sigma}$ ($\Delta T = 5$°C) under stress. At $T_{2\sigma}$, the stress is removed and the specimen is permitted to recover partially for $\Delta t_\sigma = 2$ min. The sample is then quenched to $T_o \ll T_{2\sigma}$ and viscoelastic strain ($\gamma < 10^{-3}$) is frozen in. A linear heating run at 7°C min^{-1} is then performed, during which the decay of the frozen-in strain $\gamma(t)$ is recorded. The temperature dependence of its derivative $\dot{\gamma}(T)$ constitutes an elementary TSCr spectra. Each FL response is investigated using an analysis method derived from the Bucci–Fieschi–Guidi (BFG) treatment [11] where a single retardation time for each elementary recovery process is assumed.

The retardation time τ of the isolated relaxating species as a function of time during the temperature rise is given by

$$\tau(t) = \frac{\gamma(t)}{|\dot{\gamma}(t)|} \tag{1}$$

As the time dependence of temperature is linear, $\tau(T)$ can be deduced from eqn. (1).

In polyamide blends, an Arrhenius-type dependence on temperature is assumed for the retardation time τ

$$\tau(T) = \tau_o \exp\left(\frac{\Delta H}{kT}\right) \tag{2}$$

where τ_o is the pre-exponential factor, ΔH is the apparent activation enthalpy and k is the Boltzmann constant.

RESULTS AND DISCUSSION

TSCr complex spectra

Figures 3(a) and 3(b) show the TSCr complex spectra of PA 66 and PA 66/EPR blends. For the PA 66 homopolymer, the three peaks are designated γ, β and α for increasing temperatures between −180 and 120°C. For the blends, an additional peak is observed, namely the α_E peak in the glass transition region of the EPR component [10, 12]. Values of the TSCr peak maximum temperature T_m are given in Table 1.

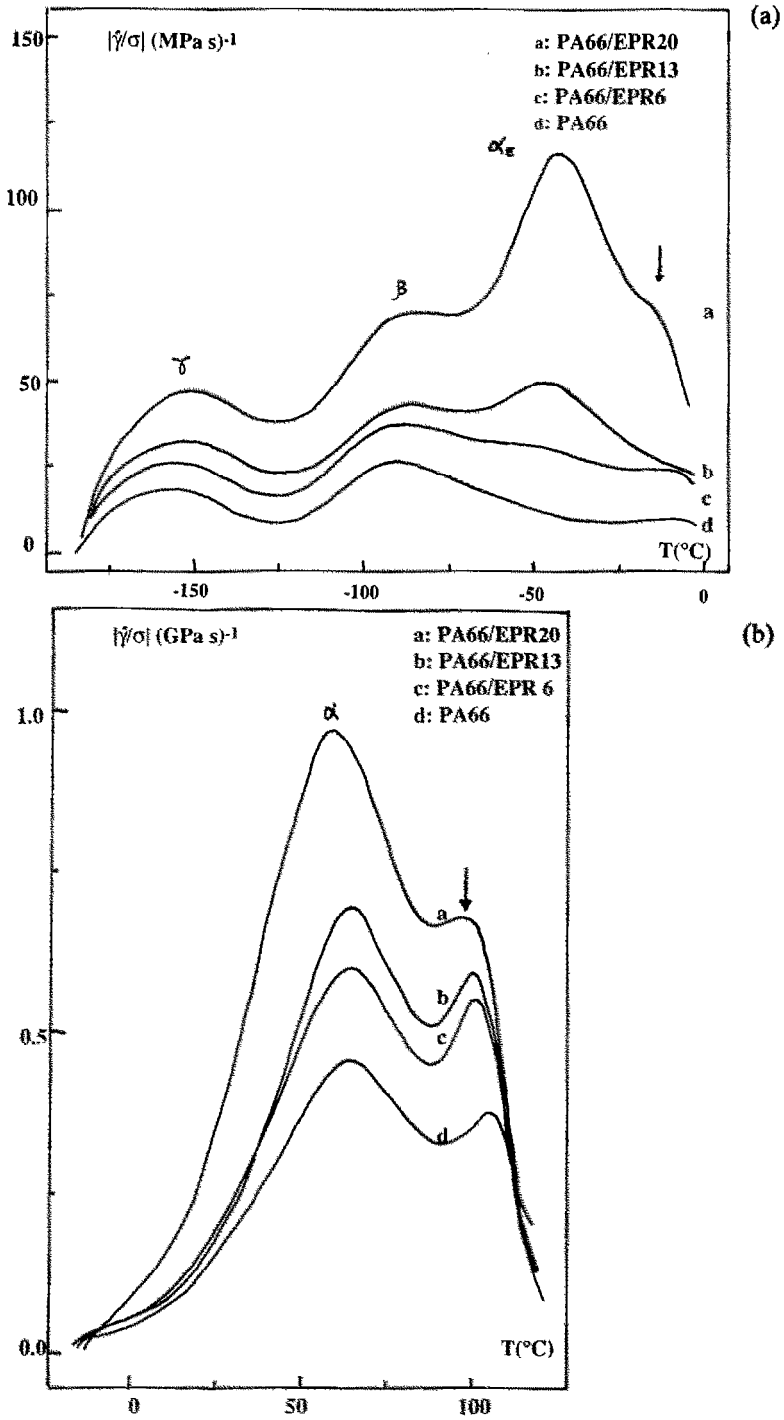

Fig. 3. (a) Low-temperature (LT) TSCr complex spectra of PA 66 and PA 66/EPR blends: T_σ (vertical arrow) = −13°C, T_o = −185°C, Δt_σ = 6 min, σ = 4.5 MPa. (b) High-temperature (HT) TSCr complex spectra of PA 66 and PA 66/EPR blends: T_σ (vertical arrow) = 97°C, T_o = −25°C, Δt_σ = 2 min, σ = 3.45 MPa.

TABLE 1

TSCr peak temperatures T_m for the γ-, β-, α_E- and α-retardation modes of PA 66 homopolymer and PA 66/EPR blends

	$T_m(\gamma)$/°C	$T_m(\beta)$/°C	$T_{m(\alpha_E)}$/°C	$T_m(\alpha)$/°C
PA 66	−155	−90	–	63
EPR 6	−153	−88	−53	65
EPR 13	−151	−86	−47	65
EPR 20	−150	−83	−43	60

With increasing EPR rubber content, the following features can be noted. The γ-TSCr peak located at about −155°C in PA 66 is almost independent of rubber content in the blends. For the β- and α_E-retardation modes, a slight shift towards higher temperatures is observed with increasing EPR rubber and, as expected, the relative height with respect to the γ- and β-relaxations is increased. The temperature position of the α-mode is independent of the rubber content in blends.

The TSCr complex spectra study of PA 66 and PA 66/EPR blends can be discussed with reference to the peak positions and the relative strengths of the retardation modes.

Fine structure of TSCr spectra

This study most be completed by an analysis of the fine structure of the retardation modes. The FL procedure was used to define more precisely the observations drawn from the complex spectra. Figures 4(a) and 4(b) show a plot of the apparent activation enthalpy as a function of T_m. T_m is taken as the maximum of each process detected by a convenient fractional stress procedure.

For clarity the fine structure of the retardation modes of the PA 66/EPR 13 blend was not plotted in the figure. From −170°C to about −60°C (Fig. 4(a)), the apparent activation enthalpy increases gradually with temperature in the PA 66, EPR 6 and EPR 20 samples. In this temperature range, no significant differences in the values of ΔH between PA 66 and PA 66/EPR blends are observed taking into account the experimental uncertainty. For higher temperatures (−50 to 0°C), the sharp increase in ΔH for the 80/20 composition is associated with the EPR glass transition region [10, 12]. This behaviour is poorly marked for the lowest rubber content (PA 66/EPR 6).

Starkweather [13] has developed a procedure to analyse the nature of viscoelastic relaxations. These relaxations are considered simple or complex depending on their activation entropies. Simple relaxations have

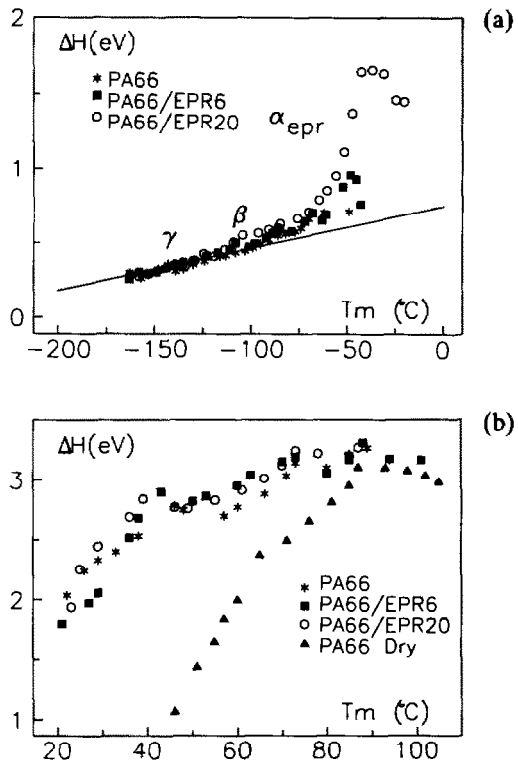

Fig. 4. (a) Apparent activation enthalpy ΔH of the γ-, β- and α_E-retardation modes of PA 66 and PA 66/EPR blends as a function of the temperature of the TSCr maximum T_m. The solid line is the Eyring–Starkweather $\Delta S = 0$ prediction. (b) Apparent activation enthalpy ΔH of the α-relaxation region of PA 66/EPR blends as a function of the temperature of the TSCr maximum T_m.

activation entropies near zero and reflect the motion of small molecular fragments without much cooperative involvement. Complex relaxations have large positive activation entropies and involve cooperative motions of neighboring groups or molecules. Starkweather concluded that the mechanical spectra of the γ- and β-modes of PA 66 may be considered as non-cooperative processes [14, 15]. An alternative to the Arrhenius equation is given by the Eyring theory of absolute reaction rates

$$f = \frac{kT}{2\pi h} \exp\left(\frac{-\Delta H}{kT}\right) \exp\left(\frac{\Delta S}{k}\right) \tag{3}$$

The Eyring activation free enthalpy ΔG can also be deduced from

$$\Delta G = \Delta H - T\Delta S = kT\left[\ln\left(\frac{k}{2\pi h}\right) + \ln\left(\frac{T}{f}\right)\right] \tag{4}$$

The solid line in Fig. 4(a) is calculated using eqn. (4) with a TSCr

equivalent frequency f of 5×10^{-3} Hz. In Fig. 4(a), up to about −90°C, a temperature range that includes the γ-mode and the onset of the β-mode, the data lie close to the relationship derived from eqn. (4) for ΔG, within experimental uncertainty, indicating that $\Delta S = 0$. In the EPR glass transition region, at the temperature $T_{m(\alpha_E)}$ of the α_E-TSCr complex peak, ΔH becomes large, as much as 2.5 times ΔG for the EPR 20 sample and only 1.5 times ΔG for EPR 6.

Starkweather [14] has examined a number of polymers with four or more methylene units. He has observed that the apparent activation entropy for γ-relaxation in dry PA 66 is much lower than in polyethylene and it becomes essentially zero in wet PA 66.

The PA 66 and PA 66/EPR samples in our study are wet, as attested by the presence of an important β-relaxation. Our results for the γ-mode confirm Starkweather's analysis. The γ-relaxation involves local movements of sequences of four or six methylene units acting in a non-cooperative manner [14]. Because the γ-relaxation in PA 66 is dielectrically active, as shown by thermally-stimulated current TSCr [16] or dielectric relaxation [15, 17, 18], the motions must involve some amide groups as well. Starkweather has determined radically different activation enthalpies from the data on the low- and high-temperature sides of the loss peaks when frequency–temperature shifting is performed for the secondary relaxation [19]. For the β-mode in wet PA 66, the low-temperature apparent activation enthalpy corresponds to an activation entropy close to zero, and the high-temperature activation enthalpies and entropies are much larger. The temperature dependence of the apparent activation enthalpies in the β-relaxation region (−125, −75°C) determined from fractional loading procedure is consistent with previous results of Starkweather.

The activation enthalpies determined from the FL procedure in the α-relaxation region are also plotted in Fig. 4(b) as a function of FL temperature of the TSCr maxima T_m. As expected, the glass transition region of PA 66 is characterized by large apparent activation enthalpies and activation entropies and is clearly a highly cooperative relaxation. Unlike the γ-, β- and α_E-relaxations, the apparent activation enthalpy of the α-relaxation is not a monotonous increasing function of T_m. Starting from the lowered T_m, ΔH rapidly increases, passes through a maximum, then through a poorly marked minimum, and increases again. The same behaviour is observed for the PA 66/EPR blends. It would seem that in this temperature range (20–80°C), two distributions in apparent activation enthalpy are present. However, it has been largely recognized that the absorbed water greatly affects the position of the relaxation [20–25] and the glass transition T_g [26]. During the fractional loading procedure performed in the α-region with T_σ varying from 12 to 82°C by steps of 5°C, the samples are drying. One may suppose that a substantial loss of water occurs during successive heating runs.

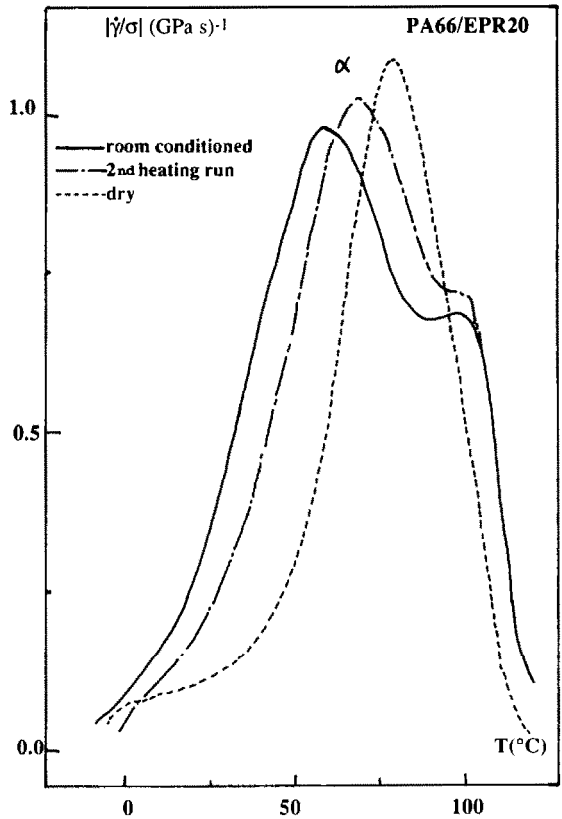

Fig. 5. Effect of in situ thermal treatment on α-TSCr peaks in PA 66/EPR 20: $T_\sigma = 97°C$, $T_o = -25°C$, $\Delta t_\sigma = 2$ min, $\sigma = 3.45$ MPa.

Figure 5 shows clearly the shift of the α-TSCr peak towards higher temperatures after three successive identical TSCr cycles in the same temperature range. Consequently, we conclude that the appearance of two distributions of ΔH in FL experiments is a result of drying the specimens. The values of ΔH between 20 and 50°C are characteristic of the α-TSCr peak in wet, ambient PA 66. Above 50°C, the apparent activation enthalpies are assigned to PA 66 in the dry state. The temperature dependence of ΔH for dry PA 66, included in Fig. 4(b), is in agreement with the preceding interpretation. One should note that the apparent activation enthalpy is higher in dry PA 66 than in wet PA 66, as has been reported for PA 6 [1] and PA 12 [23, 25].

CONCLUSIONS

The fine structure of the γ-, β- and α_E-processes in PA 66 and PA 66/EPR blends has been investigated by fractional loading experiments according to Arrhenius and Starkweather treatments. The γ-process and the low-temperature part of the β-process are well-described by the Eyring

equation using a zero activation entropy. The high-temperature part of the β-process displays weak apparent activation entropies. The apparent activation entropies are higher for the α_E-process, as expected for a relaxation associated with the glass transition of the EPR component. These entropies increase with increasing rubber content ($\Delta S = 1.2 \times 10^{-3}$ eV K^{-1} for EPR 6 and $\Delta S = 4.3 \times 10^{-3}$ eV K^{-1} for EPR 20).

The effect of water on the α-relaxation has been studied with an emphasis on the results obtained by fractional loading (FL). The two distributions in apparent activation enthalpy observed are associated with two states of humidity of PA 66: ambient wet, and dry PA 66.

REFERENCES

1 C.B. Bucknall, Toughened Plastics; Elsevier Applied Science Publishers, London, 1977.
2 S. Cimino, L. D'Orazio, R. Greco, G. Maglio, M. Malinconico, C. Mancarella, E. Martuscelli, R. Palumbo and G. Ragosta, Polym. Eng. Sci., 24 (1984) 48.
3 R.J.M. Borggreve, R.J. Gaymans, J. Shuijer and J.F. Ingen Housz, Polymer, 28 (1987) 1489.
4 C.B. Bucknall, P.S. Heather and A. Lazzeri, J. Mater. Sci., 16 (1989) 2255.
5 J. Heijboer, J. Polym. Sci. Part C, 16 (1968) 3755.
6 J.C. Radon, Polym. Eng. Sci., 12 (1972) 425.
7 E. Sacher, J. Macromol. Sci. Phys., 9 (1974) 163.
8 J.C. Monpagens, D. Chatain, C. Lacabanne and P. Gautier, Solid State Commun., 18 (1976) 1611.
9 M. Stefenel, Thesis, Paul Sabatier University, Toulouse, 1984.
10 P. Demont, D. Chatain, C. Lacabanne, D. Ronarc'h and J.L. Moura, Polym. Eng. Sci., 24 (1984) 127.
11 C. Bucci, R. Fieschi and G. Guidi, Phys. Rev., 146 (1966) 816.
12 D. Ronarc'h, P. Audren and J.L. Moura, J. Appl. Phys., 58 (1985) 474.
13 H.W. Starkweather, Macromolecules, 14 (1981) 1277.
14 H.W. Starkweather, Macromolecules, 32 (1991) 2443.
15 K. Pathmanathan, J.Y. Cavaille and G.P. Johari, J. Polym. Sci. Polym. Phys. Ed., 30 (1992) 341.
16 F. Bourret, DES Paul Sabatier University of Toulouse (1990).
17 A.J. Curtis, J. Res. Natl. Bur. Std. Sect. A, 65 (1961) 185.
18 H.W. Starkweather and J.R. Barkley, J. Polym. Sci. Polym. Phys. Ed., 19 (1981) 1211.
19 H.W. Starkweather, Macromolecules, 23 (1990) 328.
20 A.E. Woodward, J.M. Crisman and J.A. Sauer, J. Polym. Sci., 44 (1960) 23.
21 D.C. Prevorsek, R.H. Butler and H.K. Reimschuessel, J. Polym. Sci., 9 (1971) 867.
22 Y.S. Papir, S. Kapur, C.E. Rogers and E. Baer, J. Polym. Sci. Polym. Phys. Ed., 10 (1972) 1205.
23 G. Goldbach, Angew. Makromol. Chem., 32 (1973) 37.
24 J.A. Sauer and T. Lim, J. Macromol. Sci. Phys., 13 (1977) 419.
25 J. Varlet, J.Y. Cavaille and J. Perez, J. Polym. Sci. Polym. Phys. Ed., 28 (1990) 2691.
26 X. Jin, T.S. Ellis and F.E. Karasz, J. Polym. Sci. Polym. Phys. Ed., 22 (1984) 1701.